Geomechanics and Engineering, *Vol. 27, No. 1 (2021) 55-62*
https://doi.org/10.12989/gae.2021.27.1.055

An analytical approach to estimate the mechanical state of roof strata in underground longwall mining

Jie Zhang[1a], Yansong Zhang[1*], Wenzhou Du[1b], Houwang Wang[1c] and Mehdi Serati[2d]

[1]*College of Safety and Environmental Engineering, Shandong University of Science and Technology, Qingdao, 266590, China*
[2]*School of Civil Engineering, The University of Queensland, Brisbane, QLD, 4072, Australia*

(Received May 13, 2021, Revised September 21, 2021, Accepted September 28, 2021)

Abstract. The movement and collapse of roof strata in underground longwall mining is a key trigger factor for the occurrence of dynamic disasters. An accuracy estimation of roof strata mechanical state is critical for the prediction and control of dynamic disaster, such as coal burst and coal-and-gas outburst. An analytical approach is proposed in this work to estimate the mechanical state of roof strata in underground longwall mining. To do so, the unit width of roof strata is considered as a beam structure. A system of 4 simulations differential equations is proposed with 4 local slope data as input parameters to derive the mechanical expression of suspending roof strata. A differential evolution algorithm is further adapted to solve the equation system. In addition, a set of verification tests is carried out to showcase the feasibility and robustness of the proposed method. The results show that the average relative errors of 10 independent tests reach a high accuracy, which is less than 1% for the strata mechanical state control parameters. By using the estimated results, the slope, bending moment and shear force of suspending strata are derived. Moreover, the slope data sampling strategy is also devised. The parameters bound determination method is also proposed to ensure the calculation convergence. The local slope based analytical method proposed in this paper is a feasible approach to estimate the mechanical state of suspended roof strata before first weighting.

Keywords: analytical model; beam slope; differential evolution; local acceleration monitoring; longwall miningstrata mechanical state

1. Introduction

The collapse of roof strata in underground longwall mining is a dramatic strata movement mainly caused by underground pressure redistribution (Hou *et al.* 2019, Jiang *et al.* 2016, Mirenkov *et al.* 2017). The strata collapse could be a trigger that contributes to the occurrence of catastrophic dynamic disasters such as coal burst and coal-gas outburst (Keykhosropour *et al.* 2018, Li *et al.* 2017). An accurate estimation of the mechanical state of roof strata is therefore crucial for disaster early-warning, prevention and mitigation.

Numerous analytical models were proposed to explore the behaviour of roof strata. Voussoir beam as one of the most widely used models was established by Evans (1941). Brady *et al.* (2012) and Diederichs *et al.* (1999) had made their contributions to the voussoir beam model. Whittaker and Reddish (1989) derived the maximum bending moment expression of roof strata based on a simple beam model. Peng (2017) conducted extensive research on strata control in longwall mining, in which an estimation method for first and period weighting distance is proposed. Galvin (2016) suggested a series of beam models to calculate the span distance of strata. Carla (2017) found a new method to identify impending failure in rock slopes. Cetin *et al.* (2012) adopted an iterative procedure to predict the deflections at the road surface under dynamic load and designed the thickness of pavement with acceptable deflection limit. Pan *et al.* (2013) adopted the model of beam on an elastic foundation to analyse the strata behaviour and could provide a more precise formulation to indicate the loading conditions. Stolecki (2021) introduced the velocity of roof deflection as an indicator of underground workings stability. Ji *et al.* (2021) derived the mechanical state of hard roof strata by superposition method. More theories for stability analysis of beam on elastic foundations have been conducted over past decades (Koiter and van der Heijden, 2008; Timoshenko *et al.* 1962).

In relation to the monitoring methods of strata movement, the bed separation measurement method has been widely adopted in field applications (Gui *et al.* 2018). However, this method is only designated to collect data at the designed point and can be applied for a specific rock strata movement stage. That is, the bed separation measurement errors caused by unreliable reference objects are unavoidable. Matured in recent years, microseismic (MS) monitoring (Konicek 2019, Sun *et al.* 2012, Will *et al.*

∗Corresponding author, Professor
E-mail: yansongzhangskd@126.com
[a]Ph.D. Student
E-mail: zhangjieskd@hotmail.com
[b]Ph.D.
E-mail: duwenzhou-01@163.com
[c]Ph.D. Student
E-mail: whw11052512@163.com
[d]Professor
E-mail: m.serati@uq.edu.au

ISSN: 2005-307X (Print), 2092-6219 (Online)

2014), electromagnetic radiation (EMR) monitoring (Song *et al.* 2017) and acoustic emission (AE) (Hesser *et al.* 2015; Kong *et al.* 2017; Sellers *et al.* 2003) monitoring methods are feasible alternative solutions to evaluate the stability of strata. Even so, the possible unreliable and untimely result, that caused by complex data processing algorithms, as well as the exorbitant devices could pose an obstacle to large-scale adoption of those methods (Mojtaba *et al.* 2018). To the best of the authors' knowledge, there is not yet a feasible method to directly monitor the movement of roof strata.

The Local Acceleration Monitoring (LAM) (Ji *et al.* 2020, Zhang *et al.* 2018) technique, a low-cost local monitoring method that has been successfully adopted in recent years to monitor strata stability. LAM uses inertial sensors to analyse the stability of roof strata from the view of local inclinations and vibrations. The sensor chip model is MPU-6050, and it has a 3-axis gyroscope and a 3-axis accelerometer to monitor displacement and vibration. The measuring range of the accelerometer is ±16 g and the gyroscope of which is ±2000°/s. The sensor sensitivity is as high as 6.1×10-5 g within the scale range of ±2 g, and the signal frequency can be monitored from 4 Hz to 200 Hz. Since LAM is based on inertial measurements, the monitoring data will not be affected by underground reference objects, which is important for increasing the accuracy of monitoring processes. For the advantage of LAM, there is a possibility to estimate the mechanical state of suspended roof strata based on the local inclination data.
The objective of this paper is to design a scheme to estimate the strata mechanical state by using local inclination data. This scheme simplifies the strata as a beam model. The local inclination data are designated as input parameters to inverse the analysis of the mechanical state of strata. In addition, a verification test is carried out by a numerical case study to examine the robustness of the proposed method.

2. The mechanical mode of hard roof strata

2.1 The structure of roof stratum

According to the plate and shell mechanism, the roof caving configuration can be simplified as shown in Fig. 1. The highlighted area in Fig. 1 at the middle of the

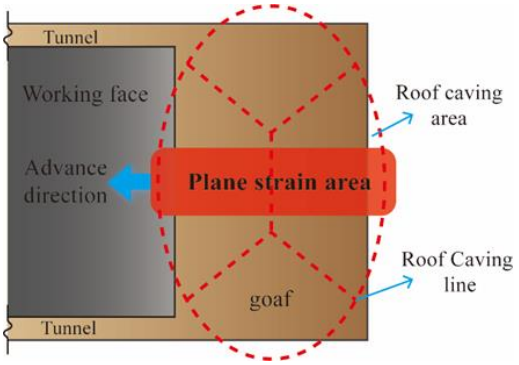

Fig. 1 Top view of roof strata caving configuration model

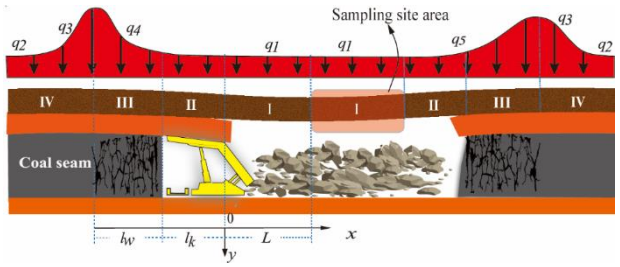

Fig. 2 Rock beam with loading and foundation mechanics model

Table 1 Rock beam mechanics conditions

Rock beam	Loading conditions	Support conditions
I	Uniformly distributed load- q_1	None
II	Increasing load- q_4 or q_5	Hydraulic support and/or residual roof
III	increasing load- q_4 or q_5	Yielded coal bed
IV	Uniformly distributed load-q_2 and decreasing load-q_3	Unyielded coal bed

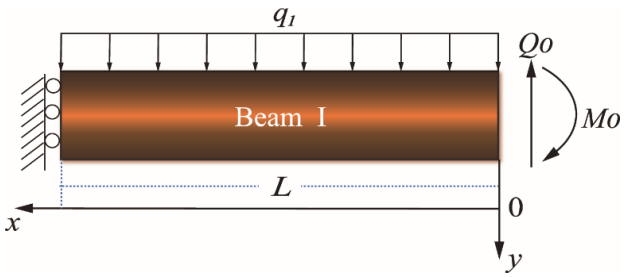

Fig. 3 Loading and boundary conditions of rock beam I

excavation is commonly regarded as a plane stain mechanical model. Therefore, the unit width of the roof strata, within the plane strain area, can be simplified as a beam structure (Yu 2016, Zhang *et al.* 2019).

The rock beam with corresponding boundary, foundations and loading conditions are displayed in Fig. 2. According to the differences in foundation support conditions, the rock beam can be divided into 4 parts, namely beam I to IV.

Based on the location of the local coordinate system shown in Fig. 2, x = L is the middle point of beam I, which can be considered as a symmetric structure. Beam I-IV with corresponding loading and support conditions are listed in Table 1.

Beam I is a suspended structure over the excavation space. Considering the field application feasibility, installation of LAM sensors in the beam I area is the most efficient scheme without too much drilling work. Therefore, beam I is selected as the slope data sampling area in this research work. The mechanical model of beam I is presented in the next section.

2.2 Mechanical model of beam I

Assuming the span of beam I is 2L, x=L is the mid-span section, the mechanical model of beam I can be simplified as a half structure. The nomination of beam I and thereafter is referred to the half structure of the whole suspended

beam. The mechanical conditions of beam I on the left side are shown in Fig. 3. The left end is a guided-support that allows deflection without any inclination. The right side is the intersection of beam I and II that represented as shear force Q_0 and bending moment M_0. The overloading is a uniformly distributed loading q_1.

In view of the loading and boundary conditions of beam I, using simple equilibrium concepts, the bending moment $M(x)$ of beam I can be derived as:

$$M(x) = M_0 - Q_0 x + \frac{1}{2} q_1 x^2 \quad (0 \le x \le L) \tag{1}$$

The slope θ(x) of beam I is:

$$\theta(x) = \frac{1}{EI}(M_0 x - \frac{1}{2} Q_0 x^2 + \frac{1}{6} q_1 x^3) + C \quad (0 \le x \le L) \tag{2}$$

where E is the plan strain modulus of strata beam, I is the area moment of inertia, C is a constant of integration. As beam I is a symmetric structure; when x=L the slope (θ) is 0 degrees and the deflection becomes the maximum, it means θ(L) = 0. According to Eq. (2), the constant of integration C can therefore be calculated as:

$$C = -\frac{1}{EI}(M_0 x - \frac{1}{2} Q_0 x^2 + \frac{1}{6} q_1 x^3) \tag{3}$$

Substituting the constant C into Eq. (2), the expression of θ can be established by:

$$\theta(x) = \frac{1}{EI}(M_0 x - \frac{1}{2} Q_0 x^2 + \frac{1}{6} q_1 x^3 - M_0 L + \frac{1}{2} Q_0 L^2 - \frac{1}{6} q_1 L^3) \quad (0 \le x \le L) \tag{4}$$

Eq. (4) is the analytical solution of slope in beam I, which indicates the functional relationship among the slope θ, the span L, the problem boundary conditions, and the bending moment M0 and shear force Q0.

3. Mechanical state estimation by inclination data

3.1 Solving mechanical system of beam I

According to Eq. (4), the mechanical state of beam I can be estimated by the solving of the L, M0, and Q0 by slope data θ.

For a certain excavation scenario, i.e. with fixed L, M0, and Q0, the slope θ can be derived by the position x. In practice, slope θ is measurable data. The sampling position x can be expressed as:

$$x = x_1 + (n-1)\Delta l_i \tag{5}$$

where parameter x1 is the distance between the first sampling site and x = 0 (the interface of rock beam I and II), Δli is the distances between the sampling sites, and n is the order of sampling site (see also Fig. 4).

Since the position x is represented by Eq. (5), there are 4 unknowns x1, L, M0 and Q0 in Eq. (4). To solve the unknowns, a system of 4 simultaneous equations is required, i.e. at least 4 inclination sensors should be installed within the beam I area. It means,

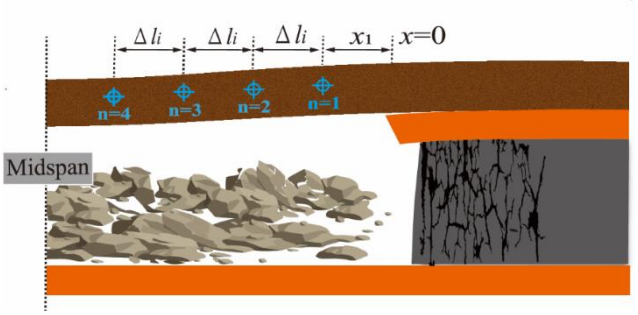

Fig. 4 The position x of sampling site

$$\begin{cases} \theta_1 = \frac{1}{EI}(M_0 x_1 - \frac{1}{2} Q_0 x_1^2 + \frac{1}{6} q_1 x_1^3 - M_0 L + \frac{1}{2} Q_0 L^2 - \frac{1}{6} q_1 L^3) \\ \theta_2 = \frac{1}{EI}(M_0 (x_1 + \Delta l_i) - \frac{1}{2} Q_0 (x_1 + \Delta l_i)^2 + \frac{1}{6} q_1 (x_1 + \Delta l_i)^3 - M_0 L + \frac{1}{2} Q_0 L^2 - \frac{1}{6} q_1 L^3) \\ \theta_3 = \frac{1}{EI}(M_0 (x_1 + 2\Delta l_i) - \frac{1}{2} Q_0 (x_1 + 2\Delta l_i)^2 + \frac{1}{6} q_1 (x_1 + 2\Delta l_i)^3 - M_0 L + \frac{1}{2} Q_0 L^2 - \frac{1}{6} q_1 L^3) \\ \theta_4 = \frac{1}{EI}(M_0 (x_1 + 3\Delta l_i) - \frac{1}{2} Q_0 (x_1 + 3\Delta l_i)^2 + \frac{1}{6} q_1 (x_1 + 3\Delta l_i)^3 - M_0 L + \frac{1}{2} Q_0 L^2 - \frac{1}{6} q_1 L^3) \end{cases} \tag{6}$$

Solving Eq. (6) by 4 slope data, the mechanical state of beam I can be achieved. For solving systems of nonlinear equations, a number of approaches have been presented. In this study, the global optimization algorithm differential evolution (DE) is adopted for its capability of solving complex equations. More discussion on the DE algorithm is presented in section 4.

3.2 Sampling strategy

Eq. (6) is derived base on the mechanical structure showed in Fig. 4, which is half of the symmetric structure. Consequently, the discussion on sampling strategy should be located on one side of the mid-span section. The mid-span section of beam I is dynamically moving forward as the span distance of beam I is increasing due to the advancement of the working face. Therefore, the sampling sites located on the left side of the mid-span should also cross the mid-span to its right side. Otherwise, it will be an invalidated site that cannot be adopted to solve equation (6). To overcome the issue, one needs to set the sampling sites to the right side of the mid-span.

In terms of the sampling interval, the theoretical ultimate span of strata (the first weighting distance) is an ideal reference length to place the sampling sites. Several theories and methods have been developed to calculate the first weighting distance. The field geological condition could be complex and the strata may collapse at a distance that is less than analytical calculated results (*Boothukuri et al*. 2019, Ning *et al.* 2020). To avoid the sampling sites becoming invalid, a conservative algorithm (Song 1988) is adopted in this study according to Eq. (7).

$$L_{\max} = \sqrt{\frac{2h_k^2 \sigma_t}{(h_k \gamma_k + \sum_{i=1}^{n} h_i \gamma_i)}} \tag{7}$$

where L_{max} is the ultimate span of the key stratum, hi and γi are the thickness and bulk density of overlying strata that

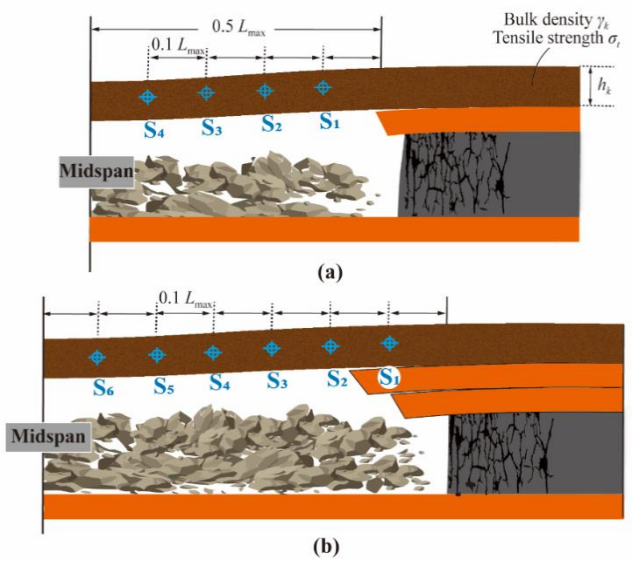

Fig. 5 Sampling sites distribution strategy

are supported by the key stratum, and σt, hk and γk are the tensile strength, thickness and bulk density of key stratum, respectively. As discussed above and given Eq. (6) is comprised of 4 independent equations, hence at least 4 sampling sites are needed to be placed. In theory, the different positions of the 4 sampling sites can be chosen arbitrarily and random, however, considering the measured errors and monitoring accuracy in practice, a uniform distribution strategy is suggested. That is, the half span of 0.5 Lmax should be divided evenly into 5 sections.

The distance between each adjacent sampling site is therefore 0.1 Lmax as shown in Figure 5a. It is worth noting that the distribution strategy showed in Figure 5a is an ideal model, and in reality, the strata caving configuration is more complex. The interface of beam I and II is unknown, hence one or more sampling sites might be located within the beam II domain, for instance the S1 site in Figure 5b. More sampling locations should be sited to overcome this difficulty, as demonstrated in Figure 5b. For this case, 6 sampling sites are suggested to be divided into 3 groups: group 1 (S1, S2, S3, S4), group 2 (S2, S3, S4, S5) and group 3 (S3, S4, S5, S6).

3.3 Bounds of the unknows

The bounds of the 4 unknowns should be given as the search range of the differential evolution algorithm. The appropriate bounds of unknowns are very essential for DE to reach the excepted result.

• Bounds of x1: According to the sampling strategy illustrated in Figure 5, the intersection of beam I and II is located between: (1) S1 and coal seam, and (2) S1 and S2. In both these two scenarios, the maximum x is 0.1 Lmax, the minimum x is 0, thus the bound of x is [0, 0.1 Lmax].

• Bounds of L: The length of beam I is smaller or equal to the working face advance distance, hence the maximum value of L can be expressed as 0.5 la, where la is the coal face advance distance. The bound of L is [0, 0.5 la].

• Bounds of M0 and Q0: Determining the bounds of bending moment M0 and shear force Q0 are complex since beam II-IV and the corresponding loading, boundary and foundation conditions should be considered carefully. In this study, analytical solutions of M0 and Q0 proposed in a peer-reviewed study (Pan *et al.* 2013) is adopted as the centre values (Mcen and Qcen) of both bounds:

$$M_{cen}=f_{c1}x_{c1}^2e\left\{\left(\frac{l_w+x_{c1}}{x_{c1}}+2\right)e^{-\frac{l_w+l_w+x_{c1}}{x_{c1}}}-\left[\frac{L+l_k+l_w+x_{c1}}{x_{c1}}+2+\frac{L+l_k}{x_{c1}}\left(\frac{L+l_k+l_w+x_{c1}}{x_{c1}}+1\right)\right]e^{-\frac{L+l_k+l_w+l_w+x_{c1}}{x_{c1}}}\right\}+\frac{q_1(L+l_k)^2}{2}-\frac{p_zl_k^2}{3} \quad (8)$$

$$Q_{cen}=f_{c1}x_{c1}e\left[\left(\frac{l_w+x_{c1}}{x_{c1}}+1\right)e^{-\frac{l_w+x_{c1}}{x_{c1}}}-\left(\frac{L+l_k+l_w+x_{c1}}{x_{c1}}+1\right)e^{-\frac{L+l_k+l_w+x_{c1}}{x_{c1}}}\right]+q_1(L+l_k)-p_zl_k \quad (9)$$

where f_{c1} and x_{c1} are the peak value adjusting parameter and the increasing rate adjusting parameter, respectively, of the increasing load q4, lk and lw are the length of beam III and rock beam II. The pz is the average supporting force. In addition, a bias of centre value 0.8 is introduced to derive the bounds with a reasonable tolerance. The bounds of M0 and Q0 are [(1-0.8) Mcen, (1+0.8) Mcen] and [(1-0.8) Qcen, (1+0.8) Qcen], respectively.

4. Differential evolution algorithm

Differential Evolution is a branch of evolutionary algorithms developed by Rainer Stron and Kenneth Price. It is a population-based direct search algorithm for global optimization capable of handling non-differentiable, non-linear and multi-modal objective functions, with few, easily chosen, control parameters (Mohamed *et al.* 2012, Omidi and Mazaheri 2020, Rout *et al.* 2013). For the advantages of the DE algorithm, it is adopted to solve the equation (6). The basic computation procedures of DE are briefly introduced in this section. In this study, a Python library, Scipy is adopted to perform the DE optimization. In terms of DE control parameters, the default setting of the Scipy DE algorithm is adopted.

4.1 Initialization

The evolution strategy of the DE algorithm starts with an initial population containing NP D-dimensional vectors. Every individual vector in the population is a set of possible values of x1, L, M0 and Q0. An individual vector is symbolized by xi,g with i = 0, 1, …, NP–1 referring to the order of a vector in a population, and g referring to the index of generation. One individual element in the vector is represented by xj,i,g with j = 0, 1, …, D-1 referring to the order of an element in a vector.

The initialization of a population (g = 0) is to choose a set of random values for each element within the given range. In this study, an element is a trail value of x1, L, M0 and Q0, and the corresponding element range is the parameter bound (bj,i,low, b j,i,up). It means,

$$\mathbf{x}_{i,0}=\left(x_{j,i,0}\right)=\mathrm{rand}_j(0,1)\left(b_{j,i,up}-b_{j,i,low}\right)+b_{j,i,low} \quad (10)$$

where rand_j (0,1) is a random number generator that returns a random number within the range [0,1). By this random number, a new random value for each element is generated,

the initial population is generated as well.

4.2 Mutation

Since the initialization population is created, the DE algorithm mutates and recombines current vectors to create NP intermediary vectors, symbolized by *vi,g*:

$$\mathbf{v}_{i,g} = \mathbf{x}_{i0,g} + F\left(\mathbf{x}_{i1,g} - \mathbf{x}_{i2,g}\right) \tag{11}$$

where $x_{i0,g}$, $x_{i1,g}$ and $x_{i2,g}$ are vectors, chosen randomly or follow certain strategy, in last generation population, F is the mutation scale factor that controls the amplification of differential variation (xi1,g – xi2,g) which also influences the convergence speed. As mutated vectors, the intermediary vectors $v_{i,g}$ not only inherit from a parent vector but also introduce differences between parent vectors.

4.3 Crossover

In order to further increase the randomness and diversity of the new vectors is introduced. Crossover operation aims to produce a trial population consist of NP trial vectors $u_{i,g}$:

$$\mathbf{u}_{i,g} = u_{j,i,g} = \begin{cases} v_{j,i,g} & \text{if } \left(\text{rand}_j(0,1) < Cr \text{ or } j = j_{\text{rand}} \right) \\ x_{j,i,g} & \text{otherwise} \end{cases} \tag{12}$$

where *Cr* is the crossover probability in the range [0,1], and rand_j (0,1) is a random number generator for the jth parameter in a vector. Increasing the value of Cr allows more parameters of intermediary vectors to progress into the next generation. Decreasing the value of Cr allows more parameters to remain unchanged. The jrand, a randomly chosen number in the range [0, D–1] to ensure the trial vectors $u_{i,g}$ will get at least one parameter from the intermediary vectors $v_{i,g}$. As a further mutation operation, the trial vectors $u_{i,g}$ inherit elements from both current vectors $x_{i,g}$ and intermediary vectors $v_{i,g}$.

4.4 Selection

Given the trial vectors ui,g and the current vector xi,g, the comparison will be carried out by substituting the parameters of the trail and current vector into the objective function. If the trial vector has an equal or better performance, the trail vector will replace the current vector in the next generation:

$$\mathbf{x}_{i,g+1} = \begin{cases} \mathbf{u}_{i,g} & \text{if } f\left(\mathbf{u}_{i,g}\right) \le f\left(\mathbf{x}_{i,g}\right) \\ \mathbf{x}_{i,g} & \text{otherwise.} \end{cases} \tag{13}$$

In this study, by repeating the mutation and competition cycle, the solved x1, L, M0 and Q0 will keep approaching to the target value, until the desired result is achieved.

5. Case study

5.1 Numerical example

A set of verification tests are carried out in this section to showcase the feasibility and robustness of the proposed method. The parameter setting reported in a peer-reviewed study (Pan *et al.* 2013) is adopted as the prototype (see also Table 2).

Table 2 Model parameters setting

Input parameter	Validation testing
Modulus of strata beam E (GPa)	25
Unit width of strata beam b_w (m)	1
Thickness of strata beam h_k (m)	6
Bulk density γ_k (kN/m^3)	25
Tensile strength of strata beam σ_t (MPa)	15
Half span of strata beam l_g (m)	20
Peak loading adjusting parameter f_{c1} (N/m)	59.55×10^6
Increasing adjusting parameter x_{c1} (m)	2
Length of rock beam III l_w (m)	10
Length of rock beam II l_k (m)	0

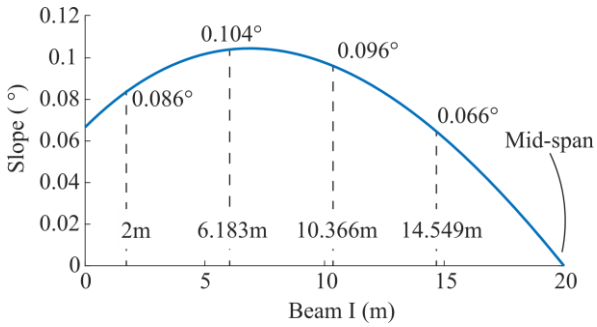

Fig. 6 Slope curve of beam I

Table 3 Parameter bounds

Parameters	Bounds	Target
x_1 (m)	[0,4.183]	2
L (m)	[0, 40]	20
M_0 (N·m)	[1.8e^7, 1.62e^8]	9e^7
Q_0 (N)	[2.9e^6, 2.6e^7]	1.46e^7

By assuming the suspended distance of strata as 40 m, the slope curve of beam I can be derived by Eqs. (4), (8) and (9), see Fig. 6.

5.2 Verification test

For the proposed mechanical state estimation approach, the input parameters are the 4 local inclination data, and the output parameters are the x_1, L, M0 and Q0.

In terms of input parameters, following the sampling strategy proposed in section 3.2, the 4 local slope data can be determined by the analytical slope solution showed in Fig. 6. As suggested by the sampling strategy, the theoretical first weighting distance is adopted to calculate the interval of sampling sites (Vecchia *et al.* 2016). In this case, by substituting the σ_t, h_k, γ_k, h_i and γ_i into equation (7) the theoretical first weighting distance L_{max} = 41.83 m, i.e., the interval of sampling sites is 4.183 m. The x1 can be

Table 4 Estimation results

Group	x (m)	L (m)	M_0 (N·m)	Q_0 (N)
1	2.06	20.14	$8.99e^7$	$1.45e^7$
2	2.48	20.55	$9.61e^7$	$1.47e^7$
3	1.80	19.87	$8.62e^7$	$1.44e^7$
4	2.09	20.16	$9.03e^7$	$1.45e^7$
5	2.09	20.16	$9.03e^7$	$1.45e^7$
6	2.37	20.44	$9.43e^7$	$1.47e^7$
7	1.89	19.96	$8.75e^7$	$1.44e^7$
8	1.97	20.04	$8.87e^7$	$1.45e^7$
9	2.10	20.18	$9.05e^7$	$1.45e^7$
10	2.15	20.22	$9.13e^7$	$1.46e^7$
Average	2.10	20.17	$9.05e^7$	$1.45e^7$
Target	2.00	20.00	$9.00e^7$	$1.46e^7$
Error	5.0%	0.85%	0.56%	0.68%

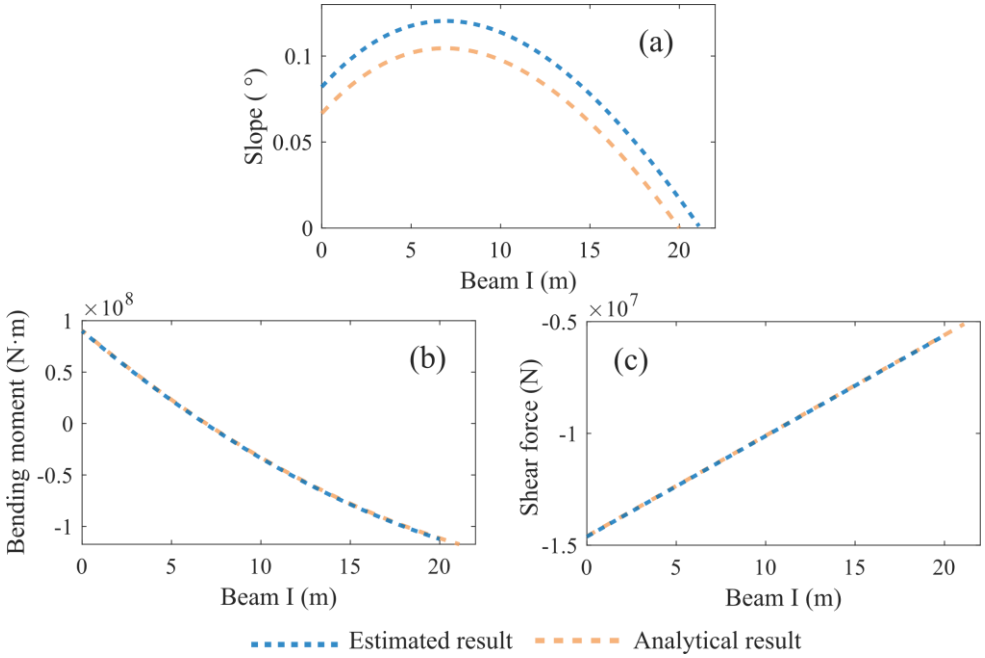

Fig. 6 Slope curve of beam I

chosen randomly ranges from 0 to 4.183 m that set to 2 m in this case study. Thus, the 4 local slope sampling sites are easily determined (see Fig. 6). To verify the performance of the proposed method, large bounds are adopted for L, M0 and Q0 as listed in Table 3.

By substituting the 4 local slope data and the output parameter bounds into the DE algorithm, a group of estimated results is derived. To eliminate the influence of singular solution, the estimation calculation is repeated 10 times, the solutions are summarized in Table 4.

The low relative error of estimated x, L, M0 and Q0 with its target value indicate the proposed approach is capable to estimate the mechanical state of beam I, the suspended strata. Moreover, the relatively large parameter bound showcases the robustness of the proposed method. By substituting the estimated L, M0 and Q0 into Eq. (1) and (2), the slope, bending moment and shear force (a derivative of M(x)) of beam I can be derived (see Figure 7).

5.3 Research limitations

The verification test shows an ideal result, whereas the proposed mechanical state estimation method is based on a simplified beam model. In practice, the overburden structure is complex having a large variation of stratum thickness and geological structure. The strata behaviour is subjected to be influenced by complex geologic conditions. A model with consideration of fault is suggested for further study.

The failure position of strata can be either in front of the working face or over goaf. The proposed method is capable to estimate the strata failure behaviour when the failure

occurs over goaf. For a comprehensive understanding of the strata movement, the mechanical model of strata over coal seam (in front of working face) is suggested to be further investigated in the further study.

The slope data are analytically calculated without errors. The resolution of slope data reaches 0.001°. However, in practice, the slope data are monitored by sensors, the errors of data caused by systematic errors and random errors are unavoidable which could pose an undesirable effect to the method. Latest studies have reported the high precision inclination sensors have been developed (Guo *et al.* 2019, Łuczak and Ekwińska 2021). A tilt sensor with 2.86×10-5 degrees resolution based on silicon-on-insulator (SOI) MEMS technology has been reported (Zou *et al.* 2014), as well as a wireless micro-electro-mechanical systems (MEMS) inclination sensor with 2.5×10-3 degrees resolution, has been applied in structural health monitoring engineering (Yu *et al.* 2009). By utilizing the latest sensor technology, the data errors are hopefully be minimized.

6. Conclusions

This paper proposed a local slope data-based analytical approach to estimate the mechanical state of roof strata. This method uses local slope data to estimate suspended span, boundary bending moment and shear force. A set of verification tests were conducted to verify the effectiveness and robustness of the proposed method. The following conclusions can be drawn from the present study. An equations system was derived for the estimation of strata mechanical behaviour. The input parameters are four (4) local slope data of strata with fixed sampling intervals. The output parameters are the sampling site positions x1, half span of suspended strata L, bending moment M0 and shear force Q0 of strata at the support boundary. The differential evolution algorithm is adopted to solve the equations system. The corresponding parameter bounds are suggested to ensure the calculation convergence. The performance of the proposed method is verified by 10 independent tests. The average relative errors of L, M_0 and Q_0 are less than 1%. By adopting the proposed method, the mechanical state of suspended strata, slope, bending moment and shear force can be estimated to higher accuracy.

Acknowledgments

The research described in this paper was financially supported by the National Natural Science Foundation of China (No. 52104201) and the Natural Science Foundation of Shandong Province (No. ZR2020QE131).

References

Boothukuri V.R., Bhattacharjee R.M., Panigrahi D.C. and Benerjee G. (2019), "Impact of geotechnical factors on strata behavior in longwall panels of Godavari Valley coal field-a case study", *Int. J. Min. Sci. Technol.*, **29**(02), 335-341. https://doi.org/10.1016/j.ijmst.2018.06.01.

Brady, B.H.G. and Brown, E.T. (2012), *Rock Mechanics: For Underground Mining*, Springer, Dordrecht, The Netherlands.

Cetin, M., Brooks, R.M. and Udo-Inyang, P. (2012), "An innovative design methodology of pavement design by limiting surface deflection", *Int. J. Recent Res. Appl. Stud.*, **13**(2), 607-610.

Carla, T., Intrieri, E., Farina, P. and Casagli, N. (2017), "A new method to identify impending failure in rock slopes", *Int. J. Rock Mech. Min. Sci.*, **93**, 76-78. https://doi.org/10.1016/j.ijrmms.2017.01.015.

Diederichs, M.S., and Kaiser, P.K. (1999), "Stability of large excavations in laminated hard rock masses: The voussoir analogue revisited", *Int. J. Rock Mech. Min. Sci.*, **36**(1), 97-117. https://doi.org/10.1016/S0148-9062(98)00180-6.

Evans, W.H. (1941), "The strength of undermined strata", *Trans. Inst. Min. Metall.*, **50**, 475-532.

Galvin, J.M. (2016), *Ground Engineering - Principles and Practices for Underground Coal Mining*, Springer Nature, Switzerland.

Gui, H.R., Tong, S.J., Qiu, W.Z. and Lin, M.L. (2018), "Research on preventive technologies for bed-separation water hazard in China coal mines", *Appl. Water Sci.*, **8**(1), 375. https://doi.org/10.1007/s13201-018-0667-0

Guo, L., Zhang, L., Song, Y., Zhao, L., and Zhao, Q. (2019), "Design and implementation of a novel tilt sensor based on the principle of variable reluctance", *Sensors*, **19**(23). https://doi.org/10.3390/s19235228.

Heijden, A.M. (2008), *W.T. Koiter's Elastic Stability of Solids and Structures*, Cambridge University Press, New York, U.S.A.

Hesser, J., Kaiser, D., Schmitz, H. and Spies, T. (2015), "Measurements of acoustic emission and deformation in a repository of nuclear waste in salt rock", *Eng. Geol. Soc. Territory*, **6**(1), 551-554. https://doi.org/10.1007/978-3-319-09060-399.

Hou, C., Zhu, W., Yan, B., Guan, K. and Niu, L. (2019), "Analytical and experimental study of cemented backfill and pillar interactions", *Int. J. Geomech.*, **19**(8). https://doi.org/10.1061/(ASCE)GM.1943-5622.0001441

Jiang, L., Mitri, H.S., Ma, N. and Zhao, X. (2016), "Effect of foundation rigidity on stratified roadway roof stability in underground coal mines", *Arab. J. Geosci.*, **9**(1), 1-12. https://doi.org/10.1007/s12517-015-2033-y.

Ji, S., Zhang, J., Pan, R. and Karlovšek, J. (2020), "Local acceleration monitoring and its application in physical modelling of underground mining", *Int. J. Rock Mech. Min. Sci.*, **128**(6), 104282. https://doi.org/10.1016/j.ijrmms.2020.104282.

Ji, S., He, H. and Karlovšek, J. (2021), "Application of superposition method to study the mechanical behaviour of overlying strata in longwall mining", *Int. J. Rock Mech. Min. Sci.*, **146**, 104874. https://doi.org/10.1016/j.ijrmms.2021.104874

Keykhosropour, L., and Lemnitzer, A. (2018), "Comparison of measurements and limit state solutions for soil pressures on deep flexible underground structures", *Geotech. Sp. Publ.*, **297**(3), 169-178. https://doi.org/10.1061/9780784481608.017.

Kong, X., Wang, E., He, X., Li, D. and Liu, Q. (2017), "Time-varying multifractal of acoustic emission about coal samples subjected to uniaxial compression", *Chaos Solitons Fractals*, **103**(1), 571-577. https://doi.org/10.1016/j.chaos.2017.07.015.

Konicek P., Schreiber J., and Nazarova L. (2019), "Volumetric changes in the focal areas of seismic events corresponding to destress blasting", *Int. J. Min. Sci. Technol.*, **29**(4), 541-547. https://doi.org/10.1016/j.ijmst.2019.06.004.

Li, L., Li, J., Sun, D. and Gong, W. (2017), "Semi-analytical approach for time-dependent load-settlement response of a jacked pile in clay strata", *Can. Geotech. J.*, **54**(12), 1682-1692. https://doi.org/10.1139/cgj-2016-0561.

Łuczak, S. and Ekwińska, M. (2021), "Electric-contact tilt sensors:

a review", *Sensors*, **21**(4). https://doi.org/10.3390/s21041097
Mirenkov, V.E., (2017), "Interaction between enclosing rocks and roof support during stoping", *J. Min. Sci.*, **53**(5), 811-817. https://doi.org/10.1134/S1062739117052813.
Mojtaba, M., Liu, H., Andrew, C., Sevda, D. and Daisuke, F. (2018), "An overview on advances in computational fracture mechanics of rock", *Geosyst. Eng.*, **3**(12). https://doi.org/10.1080/12269328.2018.1448006.
Mohamed, A.W., Sabry, H.Z., and Khorshid, M. (2012), "An alternative differential evolution algorithm for global optimization", *J. Adv. Res.*, **3**(2), 149-165. https://doi.org/10.1016/j.jare.2011.06.004.
Ning J., Wang J., Tan Y., and Qiang X. (2020), "Mechanical mechanism of overlying strata breaking and development of fractured zone during close-distance coal seam group mining", *Int. J. Min. Sci. Technol.*, **30**(2), 207-215. https://doi.org/10.1016/j.ijmst.2019.03.001
Omidi, J. and Mazaheri, K. (2020), "Differential evolution algorithm for performance optimization of the micro plasma actuator as a microelectromechanical system", *Sci. Reports*, **10**(1), 18865. https://doi.org/10.1038/s41598-020-75419-5
Pan, Y, Gu, S. and Qi, Y. (2013), "Analytic solution of tight roof's bending moment, deflection and shear force under advanced super charger load and supporting resistance before first weighting", *Chin. J. Rock Mech. Eng.*, **32**(8), 1545-1553.
Peng, S.S. (2017), *Advances in Coal Mine Ground Control, Woodhead Publishing*, Duxford, England, U.K.
Rout, U. K., Sahu, R. K., and Panda, S. (2013), "Design and analysis of differential evolution algorithm based automatic generation control for interconnected power system", *Ain Shams Eng. J.*, **4**(3), 409-421. https://doi.org/10.1016/j.asej.2012.10.010.
Sellers, E.J., Kataka, M.O. and Linzer, L.M. (2003), "Source parameters of acoustic emission events and scaling with mining-induced seismicity", *J. Geophys. Res. Solid Earth*, **108**(B9), 24, 003. https://doi.org/10.1029/2001JB000670.
Song, Z. (1988), *Utility mine Pressure and Control*, China University of Mining and Technology Press, Xu Zhou, China.
Song, D., Wang, E., Li, Z., Qiu, L. and Xu, Z. (2017), "EMR: An effective method for monitoring and warning of rock burst hazard", *Geomech. Eng.*, **12**(1), 53-69. https://doi.org/10.12989/gae.2017.12.1.053.
Sun, J., Wang, L. and Hou, H. (2012), "Application of micro-seismic monitoring technology in mining engineering", *Int. J. Min. Sci. Technol.*, **22**(1), 79-83. https://doi.org/10.1016/j.ijmst.2011.06.007.
Stolecki, L. and Grzebyk, W. (2021), "The velocity of roof deflection as an indicator of underground workings stability – Case study from Polish deep copper mines", *Int. J. Rock Mech. Min. Sci.*, **143**, 104717. https://doi.org/10.1016/j.ijrmms.2021.104717.
Timoshenko, S.P., Gere, J.M. and Prager, W. (1962), "Theory of elastic Stability, second edition", *J. Appl. Mech.*, **29**(1), 220-221. https://doi.org/10.1115/1.3636481.
Vecchia, G.D., Bellis, M.L.D. and Pandolfi, A. (2016), "A multiscale microstructural model of damage and permeability in fractured solids", *Proc. Eng.*, **158**, 21-26. https://doi.org/10.1016/j.proeng.2016.08.399.
Whittaker, B.N. and Reddish, D. J. (1989), Subsidence: Occurrence, Prediction and Control, Elsevier Science Publishers B.V, The Netherlands.
Will, R., Smith, V., Leetaru, H. E., Freiburg, J. T., and Lee, D. W. (2014), "Microseismic monitoring, event occurrence, and the relationship to subsurface geology", *Energy Procedia*, **63**, 4424-4436. https://doi.org/10.1016/j.egypro.2014.11.478.
Yu, B. (2016), "Behaviors of overlying strata in extra-thick coal seams using top-coal caving method", *J. Rock Mech. Geotech. Eng.*, **8**(2), 238-247. https://doi.org/10.1016/j.jrmge.2015.11.006.
Yu, Y., Ou, J., Zhang, J, Zhang, C. and. Li, L. (2009), "Development of wireless MEMS inclination sensor system for swing monitoring of large-scale hook structures", *IEEE T. Industr. Electronics*, **56**(4), 1072-1078. https://doi.org/10.1109/TIE.2009.2012469.
Zhang J., Yang W., Lin B., Zhang J. and Wang M. (2019), "Strata movement and stress evolution when mining two overlapping panels affected by hard stratum", *Int. J. Min. Sci. Technol.*, **29**(5), 691-699. https://doi.org/10.1016/j.ijmst.2019.07.001
Zhang, K., Ji, S., Zhang, Y., Zhang, J. and Pan, R. (2018), "MEMS inertial sensor for strata stability monitoring in underground mining: an experimental study", *Shock Vib.*, (6), 1-8. https://doi.org/10.1155/2018/4895862.
Zou, X., Thiruvenkatanathan, P. and Seshia, A. A. (2014), "A high-resolution micro-electro-mechanical resonant tilt sensor", *Sensors Actuators A Phys.*, **220**, 168-177. https://doi.org/10.1016/j.sna.2014.10.004.

IC